Multidisciplinary Analysis of the NEXUS Precursor Space Telescope

Olivier L. de Weck[a], David W. Miller[a] and Gary E. Mosier[b]

[a] Department of Aeronautics & Astronautics, Engineering Systems Division (ESD),
Massachusetts Institute of Technology, 77 Massachusetts Avenue, Cambridge, MA 02139
[b] NASA Goddard Space Flight Center, Greenbelt, MD 20771

ABSTRACT

A multidisciplinary analysis is demonstrated for the NEXUS space telescope precursor mission. This mission was originally designed as an in-space technology testbed for the Next Generation Space Telescope (NGST). One of the main challenges is to achieve a very tight pointing accuracy with a sub-pixel line-of-sight (LOS) jitter budget and a root-mean-square (RMS) wavefront error smaller than $\lambda/50$ despite the presence of electronic and mechanical disturbance sources. The analysis starts with the assessment of the performance for an initial design, which turns out not to meet the requirements. Twentyfive design parameters from structures, optics, dynamics and controls are then computed in a sensitivity and isoperformance analysis, in search of better designs. Isoperformance allows finding an acceptable design that is well "balanced" and does not place undue burden on a single subsystem. An error budget analysis shows the contributions of individual disturbance sources. This paper might be helpful in analyzing similar, innovative space telescope systems in the future.

Keywords: Space Telescopes, NEXUS, Isoperformance, Dynamics and Controls, Spacecraft Design, Optics, Sensitivity Analysis

1. INTRODUCTION

The quest for better angular resolution $\theta = \lambda/D$, greater photon collection area D^2 and a low disturbance environment invariably leads to large optical systems in space. In order to be accommodated within current launch vehicle fairing constraints (max $\sim$ 4-5 meter diameter), see Fig.1(a), such systems are forced to be lightweight, deployable and consequently very flexible. The task of imaging faint targets (long exposure times) with such flexible telescopes poses challenges for keeping the line-of-sight (LOS) pointing errors and the wavefront error distortions due to dynamical disturbances to a minimum. Also, one may expect much tighter coupling between the following disciplines: structures, optics and controls. This paper presents the results of a multidisciplinary analysis for the NEXUS space telescope. The analysis follows the methodology previously developed as part of the DOCS* framework.[1]

This paper first provides a description of the NEXUS spacecraft as well as the underlying integrated model. A disturbance analysis (= performance assessment) is then carried out for an initial design. This design is expressed as a vector, p_o, of 25 system parameters. These variables represent selected disturbance, plant, optics and controls parameters of the system. After establishing that the initial design does not meet the performance requirements for wavefront error ($J_{z,1}$ =RMMS WFE) and line-of-sight jitter ($J_{z,2}$ =RSS LOS), a sensitivity analysis is conducted in order to obtain the Jacobian, ∇J_z, where $J_z = [J_{z,1} \ J_{z,2}]^T$. This information is then used in a bivariate and multivariable isoperformance analysis which computes contours of acceptable performance $J_{z,req} = [20\text{nm} \ 5\mu\text{m}]^T$. This is different from system optimization, where one would seek the best-possible performance given a set of constraints. Here we search for a set of *acceptable* designs that balance the degree of difficulty across subsystems. Finally, error budgeting is presented as a means of understanding the contribution of individual noise sources to the total error. The purpose of this paper is to demonstrate the usefulness of the DOCS framework on a realistic conceptual design model of a high-performance spacecraft.

Further author information: deweck@mit.edu, Telephone: 1 617 253 0255
*DOCS=Dynamics-Optics-Controls-Structures

2. NEXUS DESCRIPTION

NEXUS features a 2.8 m diameter primary mirror, consisting of three primary mirror (PM) petals, which are the size of NGST's Advanced Mirror System Demonstrators (AMSD). Two of these are fixed and one is deployable as shown in Figure 1(a) on the left side. The assumed operating wavelength is $\lambda = 1$ [μm]. The total mass of the spacecraft is nominally 810 [kg] at a cost of $M 105.88 (FY00), which includes launch and mission operations. The expected power consumption is 225 [W] and the target orbit is the Lagrange point L2 of the Sun/Earth system with a projected launch date of 2004[†]. The optical telescope assembly (OTA) also features a 3-legged spider, which supports the secondary mirror (SM). The instrument module contains the optics downstream of the tertiary mirror and the camera (detector). The sunshield is large, deployable and accounts for the first flexible mode of the spacecraft structure around 0.2 Hz.
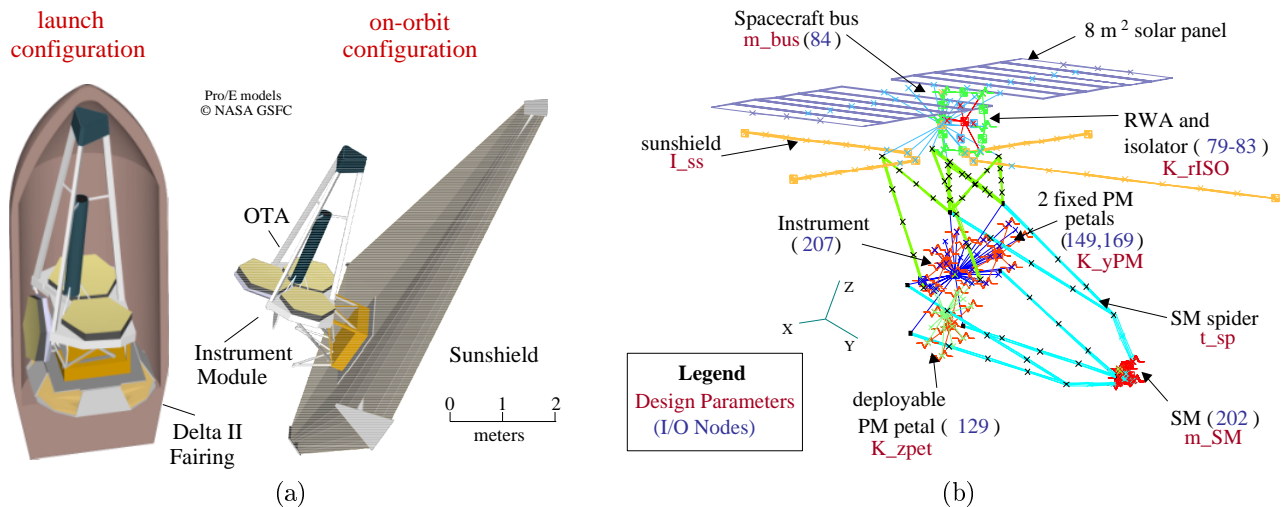

Figure 1. (a) NEXUS Spacecraft Concept in launch configuration (left) and deployed on-orbit configuration (right). (b) NEXUS Finite Element Model. Important I/O grid points (node numbers in parentheses) and variable design parameters are shown.

The challenge at a systems level is to find a design that will meet optical performance requirements in terms of pointing and phasing of the science light. This has to be done taking into account the flexible dynamics of the system, the control loops for attitude and pointing as well as the on-board mechanical and electronic noise sources. The following analyses are carried out in order to find a well "balanced" design, using the isoperformance technique.[2]

2.1. Finite Element Model

The integrated model for NEXUS contains a structural finite element model (FEM) in the deployed configuration, see Figure 1(b). The model was initially created in FEMAP/NASTRAN and subsequently translated to IMOS.[3] The advantage of IMOS is that it can easily manipulate the model for parametric trade studies (such as isoperformance) in MATLAB, whereas NASTRAN is better suited for the analysis of large, high-fidelity point designs. This model features 273 grid points, 678 independent degrees-of-freedom after Guyan reduction and is optimized for use as a dynamics model below ~ 100 [Hz]. Figure 1(b) shows the important locations at which disturbance and control inputs enter as well as important output nodes for the ACS as well as the locations where optical elements are mounted. This FEM is used to obtain a state space representation of the plant, see " Nexus Plant Dynamics" block in Fig.4. The variable FEM parameters are shown in Table 1 as "plant parameters".

2.2. Optics Model

The Cassegrain optics of NEXUS consist, among others, of a three petal primary mirror with an equivalent diameter of 2.8 [m]. Two of the petals are fixed (PM segments #2 and 3) to the primary optical bench, while the third petal (PM segment #1) is deployable. The hinge stiffness, $K_z pet$, of the deployable petal is one of the variable design parameters considered in Table 1. The light from distant science targets and guide stars is

---

[†]NEXUS was cancelled as part of the NGST rescoping effort in December 2000.

then reflected from the concave primary and directed towards the convex secondary mirror (SM). Note that the optical boresight axis in the optics model (ZEMAX) is in the +z direction, see Figure(2a). The back end optics consist of a fold mirror, a focal tertiary mirror, a deformable mirror (DM), a flat fast steering mirror (FSM), several dichroics and camera fold mirrors and, finally, the exit pupil and the detector focal plane. A ray tracing diagram of the NEXUS optical train is shown in Figure 2. The optical prescription contains a total of 20 optical elements, including the source reference plane (object) and the detector focal plane (image).
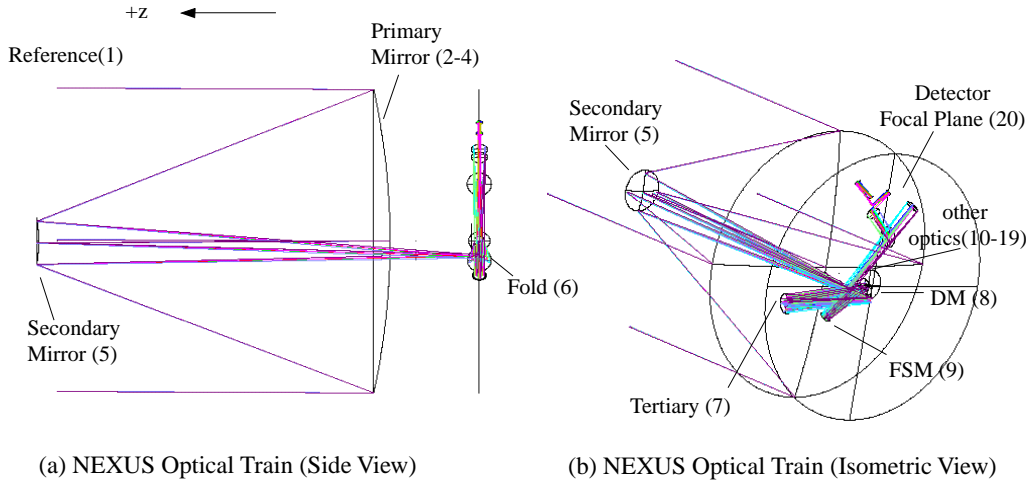

(a) NEXUS Optical Train (Side View)   (b) NEXUS Optical Train (Isometric View)

Figure 2. NEXUS Optical Train modeled with ZEMAX. (a) Side View. (b) Isometric View. Selected mirror surfaces are labeled according to their element number (`iElt`) in the NEXUS OTA prescription. Key optics data: PM f/#=1.25, Magnification M=12, back focal length BFL=0.2 [m], SM diameter 0.27 [m], f/15 beam at Cassegrain focus, f/24 telescope at focal plane, same as NGST. Plate scale = 2.06 [masec/μm].

Ray tracing according to the method developed by Redding and Breckenridge[4] is used to characterize the effect of perturbations in the positions and rotations of the optical elements. The motion of optical elements affects the image quality of NEXUS. This effect is characterized by the dependence of the image centroid and wavefront error on the translation and rotation of optical components. The two performance metrics of interest are the root-mean-mean-square wavefront error, $J_{z,1}$ = RMMS WFE, and the root-sum-square line-of-sight jitter, $J_{z,2}$ = RSS LOS. The optical linear sensitivity matrices for these performances with respect to the translations and rotations of the optical elements were computed with MACOS, see Reference[5] for details. The wavefront error and centroid are then computed with the following, linearized relationships:

$$W_i = W_{o,i} + \sum_{j=1}^{n_{dof}} \frac{\partial W_i}{\partial u_j} \cdot \Delta u_j \quad \text{where } i = 1, 2, \ldots, n_{rays}$$
$$C_x = \sum_{j=1}^{n_{dof}} \frac{\partial C_x}{\partial u_j} \cdot \Delta u_j \text{ and } C_y = \sum_{j=1}^{n_{dof}} \frac{\partial C_y}{\partial u_j} \cdot \Delta u_j \tag{1}$$

where $W_{o,i}$ is the residual design wavefront error of the i-th ray, $\partial W / \partial u$, is the wavefront sensitivity matrix, u is a vector of displacements and rotations and $\partial C / \partial u$ is the centroid linear sensitivity matrix. A total of n_{rays}=1340 rays are used for the analysis. The RMMS metric averages the W_i's over the entire light bundle, while the LOS jitter metric is the root-sum-squared (RSS) of C_x and C_y.

2.3. Disturbance Sources

There are four expected disturbance sources in the NEXUS integrated model ($n_d = 4$). The first is broadband reaction wheel noise, assuming a 4-wheel pyramid and uniform probability density on the wheel speed distribution, with an upper (operational) wheel speed R_u. The disturbance forces and torques are caused by static and dynamic imbalances, U_s and U_d, as well as higher harmonics.[6,7] Figure 3 shows the typical "sawtooth" pattern of the broadband disturbance PSD's for a single wheel along with low-order state space overbounds. This allows including pre-whitening filters in the overall state space system, S_{zd}.

The second disturbance is due to a linear Sterling cryocooler at drive frequency f_c. This device is used to cool the IR detector and is installed in the instrument module. The third disturbance is attitude noise, which is based on rate gyro noise and star tracker noise measured on the Cassini mission (JPL). Finally there is guide star noise, which is very sensitive to the guider sampling rate, T_{gs}, and the guide star brightness, M_{gs}.
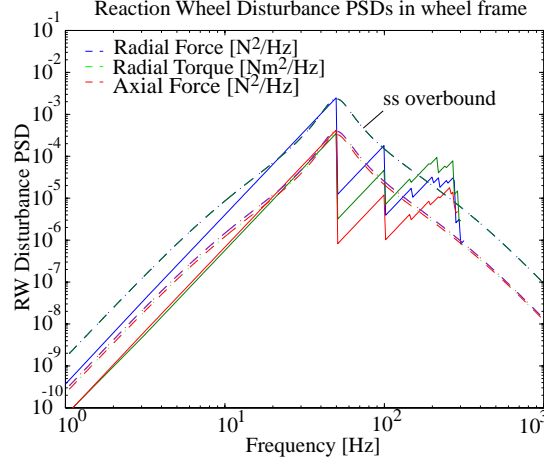
Figure 3. NEXUS broadband reaction wheel disturbance model. Nominal parameters: $R_u = 3000$ [RPM], $U_s = 0.7160$ [gcm] and $U_d = 29.536$ [gcm^2].

2.4. Appended Dynamics and Controls

The appended dynamics of this system are shown in the block diagram of Figure 4. These dynamics have also been cast in an equivalent state space form, S_{zd}, as shown in Eq. 2. Note that the subscripts refer to the respective subsystem dynamics: dw reaction wheel disturbance, dc cryocooler disturbance, ds ACS sensor noise, dg guide star noise, p structural plant, ca ACS controller and cf for the FSM controller. The way in which such integrated models are assembled and conditioned in state space form is described elsewhere.[2]

$$
\dot{q}_{zd} = \begin{bmatrix}
A_{dw} & 0 & 0 & 0 & 0 & 0 & 0 \\
0 & A_{dc} & 0 & 0 & 0 & 0 & 0 \\
0 & 0 & A_{ds} & 0 & 0 & 0 & 0 \\
0 & 0 & 0 & A_{dg} & 0 & 0 & 0 \\
B_{p1}RC_{dw} & B_{p2}C_{dc} & 0 & 0 & A_p & B_{p3}C_{ca} & 0 \\
0 & 0 & B_{ca2}C_{ds} & 0 & B_{ca}C_p & A_{ca} & B_{ca3}C_{cf} \\
0 & 0 & 0 & B_{cf}C_{dg} & B_{cf}\frac{\partial C}{\partial u}C_{p1} & 0 & A_{cf} - B_{cf}K_{fsm}C_{cf}
\end{bmatrix} q_{zd}
$$
$$
+ \begin{bmatrix}
B_{dw} & 0 & 0 & 0 \\
0 & B_{dc} & 0 & 0 \\
0 & 0 & B_{ds} & 0 \\
0 & 0 & 0 & B_{dg} \\
0 & 0 & 0 & 0 \\
0 & 0 & 0 & 0 \\
0 & 0 & 0 & 0
\end{bmatrix} \begin{bmatrix}
d_{RWA} \\
d_{Cryo} \\
d_{ACS} \\
d_{FGS}
\end{bmatrix}
$$
$$
z = \begin{bmatrix}
0 & 0 & 0 & 0 & \frac{\partial W}{\partial u}C_{p1} & 0 & 0 \\
0 & 0 & 0 & 0 & \frac{\partial C}{\partial u}C_{p1} & 0 & -K_{fsm}C_{cf}
\end{bmatrix} q_{zd} + [0]_{1340x10}\, d
$$

(2)

In summary the appended dynamics, S_{zd}, of this system contain 320 states ($n_s = 320$), two performance metrics ($n_z = 2$), four disturbance sources ($n_d = 4$) and 25 variable design parameters ($n_p = 25$). Note that variable disturbance, structural, optics and control parameters are considered simultaneously. Mostly one finds subsets such as controls/structures in the literature, but with the assumption of fixed noise sources. Table 1 summarizes the variable design parameters in this study.

3. DISTURBANCE ANALYSIS

A disturbance analysis (=performance assessment) of the science target observation mode was carried out with the initial parameters, p_o, given in Table 1. Results for LOS jitter are contained in Figure 5(a). The bottom plot shows a sample time realization for 5 seconds and the centroid X location, C_x. The middle plot shows the PSD of LOS jitter ($J_{z,2}$ =RSS LOS=$\sqrt{C_x^2 + C_y^2}$). The top plot is the cumulative RSS of LOS jitter as a function of frequency. One can see that a mode at 23 [Hz] contributes most significantly to LOS jitter (secondary tower bending). The group of highly damped modes in the region from 10-20 [Hz] represents the RWA isolator dynamics.

Another way to look at performance $J_{z,2}$=RSS LOS is to plot the time histories from the motions of centroid X and Y versus each other. This has been done in Figure 5(b). The predicted RSS LOS is 14.97 μm, versus a

Figure 4. NEXUS block diagram with 4 disturbance sources (RWA, Cryo, ACS noise, GS noise) and 2 performances (RMMS WFE, RSS LOS). Simulation implemented in Simulink as well as state space.

Table 1. NEXUS Variable Design Parameters p_j, $j = 1, \ldots, 25$.

Number	Symbol	Nominal	Description	Units
			disturbance parameters	
1	Ru	3000	Upper operational wheel speed	[RPM]
2	Us	1.8	Static wheel imbalance	[gcm]
3	Ud	60	Dynamic wheel imbalance	[gcm^2]
4	fc	30	Cryocooler drive frequency	[Hz]
5	Qc	0.005	Cryocooler attenuation factor	[-]
6	Tst	20	Star tracker update rate	[sec]
7	Srg	3e-14	Rate gyro noise intensity	[rad^2/s]
8	Sst	2	Star tracker one sigma	[arcsec]
9	Tgs	0.04	Guider integration time	[sec]
			plant parameter	
10	m_{SM}	2.49	mass of secondary mirror	[kg]
11	K_yPM	0.8e6	Primary mirror bipod stiffness	[N/m]
12	K_rISO	3000	RWA Isolator joint stiffness	[Nm/rad]
13	m_{bus}	0.3e3	Spacecraft bus mass	[kg]
14	$Kzpet$	0.9e8	PM petal hinge stiffness	[N/m]
15	t_{sp}	0.003	Spider wall thickness	[m]
16	I_{ss}	0.8e-8	Sunshield bending inertia	[m^4]
17	$I_{prop}t$	5.11	Propulsion system inertia	[kgm^2]
18	ζ	0.005	modal damping ratio	[-]
			optics parameters	
19	λ	1e-6	Centerline optical wavelength	[m]
20	Ro	0.98	Optical surface reflectivity	[-]
21	QE	0.80	CCD quantum efficiency	[-]
22	Mgs	15.0	Magnitude of guide star	[mag]
			controls parameters	
23	fca	0.01	ACS control bandwidth	[Hz]
24	Kc	0.0	FSM/ACS coupling gain	[0-1]
25	Kcf	2000	FSM controller gain	[-]

requirement of 5 μm[‡]. Note that the RSS of the centroid jitter is larger than the size of a single pixel (25 × 25 μm), which is undesirable.

The wavefront error performance is omitted here for simplicity. Table 2 shows an overview of the predicted

[‡]This requirement comes from the assumption of 25 μm pixel pitch and a desire to maintain LOS jitter below 1/5 of a pixel.
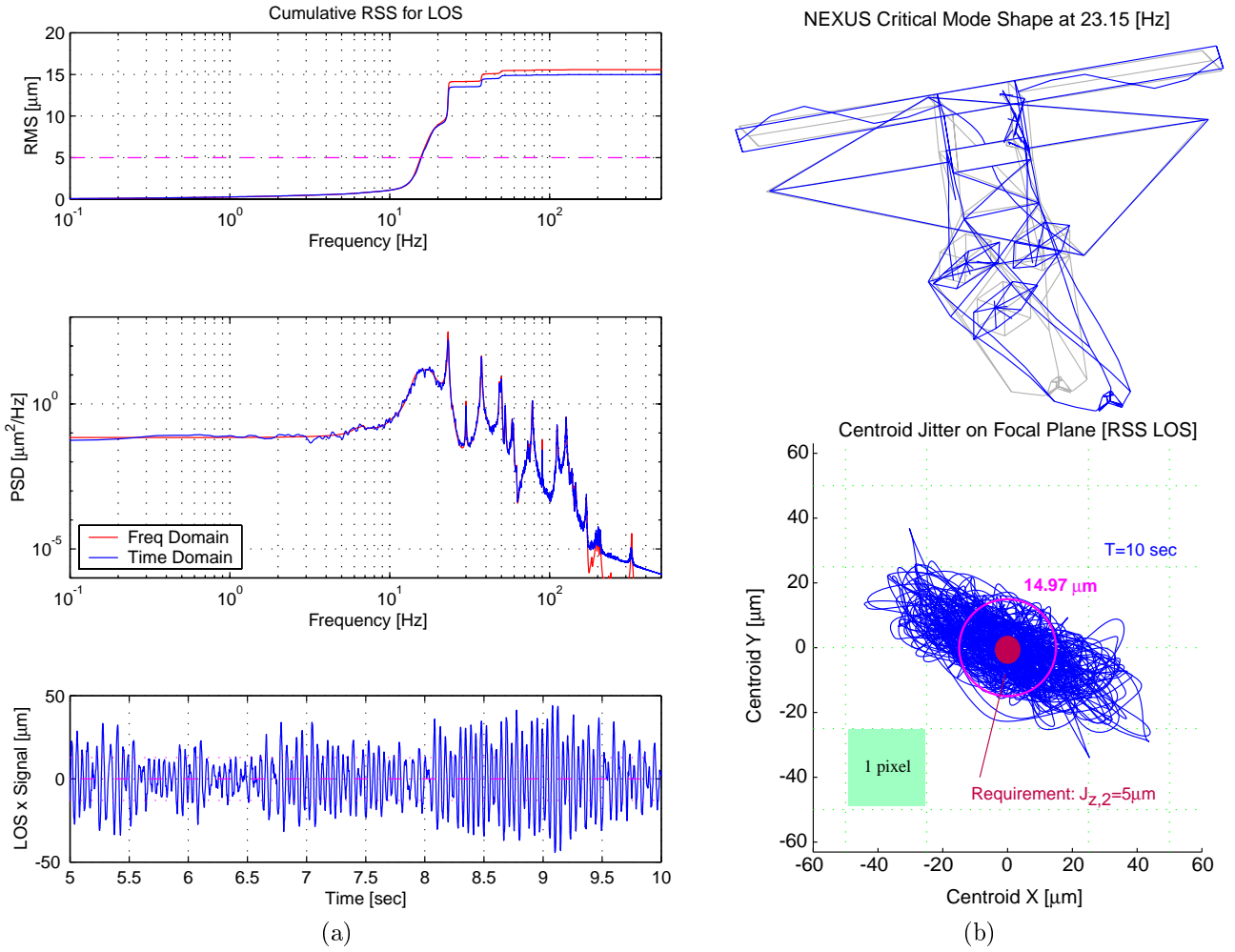
Figure 5. (a) LOS Jitter initial disturbance analysis with time domain sample realization (bottom), PSD (middle) and cumulative RSS plot (top). (b) RSS LOS Centroid Jitter Plot on Detector Focal Plane (`iElt=20`) - bottom. Mode Shape of critical mode at 23.15 [Hz] - top.

Table 2. Initial Performance Analysis Results

Performance	Lyapunov	Time Domain	Requirement	Units
$J_{z,1}$ RMMS WFE	25.61	19.51	20	[nm]
$J_{z,2}$ RSS LOS	15.51	14.97	5	[μm]

performance, using the initial parameters p_o. The wavefront error requirement ($\lambda/50$) is nearly met, but the pointing performance has to improve by a factor of roughly 3. This is not atypical for many systems with multiple performances ($n_z > 1$), where only a subset of performance requirements is initially close to being met. The next step is to conduct a sensitivity analysis. The goal is to understand with respect to which parameters p_j the performances $J_{z,i}$ are most sensitive to. The partial derivatives $\partial J_{z,1}/\partial p_j$ and $\partial J_{z,2}/\partial p_j$ will give this insight.

4. SENSITIVITY ANALYSIS

This section shows the results of a comprehensive sensitivity analysis for the 25 variable design parameters of NEXUS which are shown in Table 1. The sensitivity produces the normalized Jacobian matrix (25×2 matrix) evaluated at p_o. Details of sensitivity analysis are discussed by Gutierrez.[8]

$$\overline{\nabla} J_z = \frac{p_o}{J_{z,o}} \begin{bmatrix} \dfrac{\partial J_{z,1}}{\partial R_u} & \dfrac{\partial J_{z,2}}{\partial R_u} \\ \cdots & \cdots \\ \dfrac{\partial J_{z,1}}{\partial K_{cf}} & \dfrac{\partial J_{z,2}}{\partial K_{cf}} \end{bmatrix} \tag{3}$$

This is graphically shown in Figure 6. Note that parameters Ru through Tgs are disturbance parameters, m_{SM} through $zeta$ are structural plant parameters, $lambda$ through Mgs are optical parameters and fca through Kcf are control parameters. These parameters were first described in Table 1.
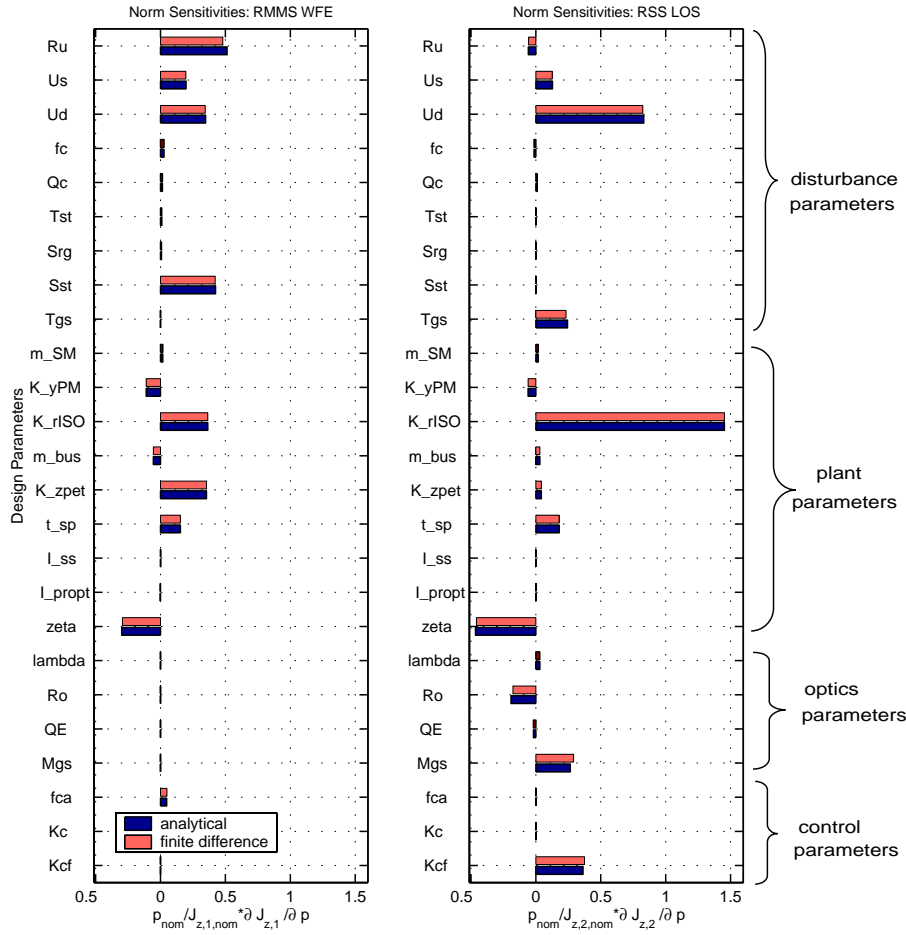
Figure 6. NEXUS normalized sensitivity analysis results at p_o using the analytical and finite difference methods.[8]

The RMMS WFE is most sensitive to the upper operational wheel speed, Ru, the RWA isolator stiffness, $K_r ISO$, and the deployable petal hinge stiffness, $K_z pet$. The RSS LOS is most sensitive to the dynamic wheel imbalance, Ud, the RWA isolator stiffness, $K_r ISO$, structural damping, $zeta$, the guide star magnitude, Mgs and the FSM (fine pointing loop) control gain, Kcf. Interpreting these results one would expect for example that a 1.0 % decrease in the isolator stiffness, $K_r ISO$ should lead to roughly a 1.5 % decrease in LOS jitter. The sensitivity analysis can be used to select a subset of interesting parameters for further analysis and redesign.

5. ISOPERFORMANCE ANALYSIS

In classical design optimization one attempts to find the best possible system performance, J_z, given a set of constraints on the system parameters p_j. Isoperformance on the other hand tries to drive the system performance

towards the specified requirement $J_{z,req}$ but not any better, since a further increase in performance is not warranted by the specification and will likely come at a significant increase in cost (better sensors, more power consumption for controllers etc...). Mathematically finding the isoperformance set corresponds to determining the n_p-dimensional isoperformance contours.

5.1. Imbalance versus Isolation

A bivariate isoperformance analysis is conducted for NEXUS using $J_{z,2}$ = RSS LOS as the performance and the two most sensitive parameters from Figure 6, right column, as the parameters. Hence, dynamic wheel imbalance, Ud, is traded versus RWA isolator joint stiffness, K_rISO, while constraining the performance to the requirement, $J_{z,2,req} = 5$ [μm]. A graphical representation of these two variable parameters in the context of the NEXUS spacecraft bus design is shown in Figure 7.
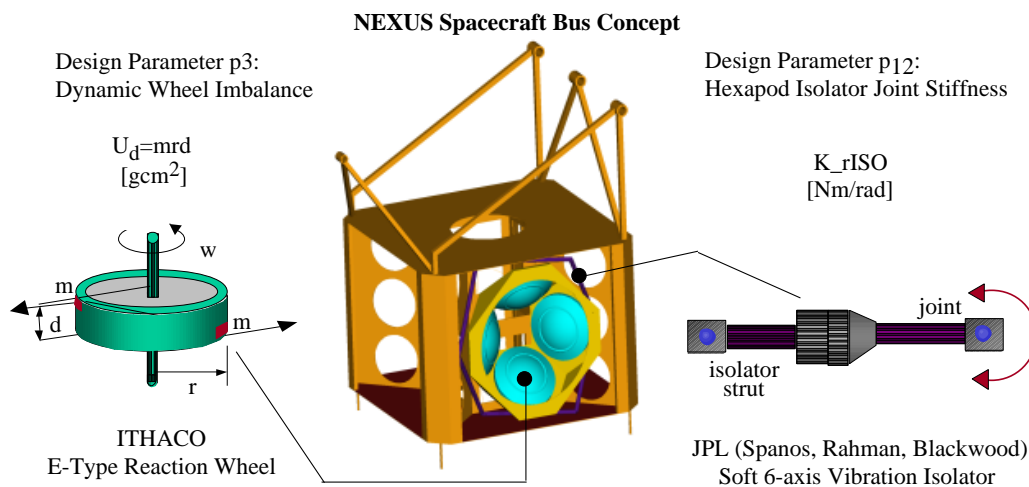

Figure 7. NEXUS Bus design with a 4-wheel symmetric pyramid of ITHACO E-wheels (39.3 [cm] diameter, 16.6 [cm] height, 10.6 [kg] mass each). See Reference[9] for 6-axis Active Vibration Isolator design.

The isoperformance contours (Figure 8) were obtained using the search algorithm developed by de Weck.[10] This analysis required 1506.2 [sec] of CPU time (Pentium III, 650 MHz processor) and a total of $2.51 \cdot 10^{11}$ FLOPS. The use of a fast, diagonal Lyapunov solver[11] causes the FEM (mass and stiffness) assembly time to be the most time consuming operation instead of the solution of the Lyapunov equation for the state covariance matrix, Σ_q.
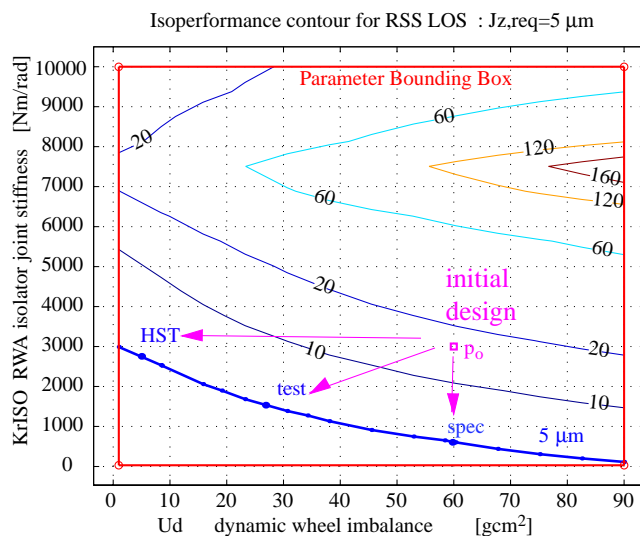

Figure 8. NEXUS Bivariate Isoperformance analysis with $p_3 = U_d$, $p_{12} = K_rISO$ and $J_{z,2}$ =RSS LOS.

The isoperformance contour at RSS LOS = 5 [μm] can be reached from the initial design, p_o, by keeping the same amount of imbalance in the wheels (specification value of E-wheel: $U_d = 60$ [gcm^2]) and softening the isolator to below 1000 [Nm/rad], thus reducing the isolator corner frequency to roughly 1.2 Hz. Alternatively the isolator can remain the same and the imbalance could be reduced to close to its lower bound, U_d=1 [gcm^2]. The isoperformance contour passes through these two points, so a combination of the above is likely to also result in the desired effect. Note that the performance degrades significantly for stiffer isolator joints and larger imbalances. The region in the upper right of Figure 8, where LOS jitter of 160 μm is predicted, occurs, when the isolator modes coincide with other flexible modes of the NEXUS structure.

5.2. Multivariable Isoperformance

Since isoperformance solutions do not distinguish themselves via their performance, we may satisfy some additional objectives. For the bivariate analysis of U_d versus $K_r ISO$ it is not immediately clear whether it is more favorable or "expensive" to improve the balancing of the reaction wheels or to build a "softer" hexapod isolator. Once the (iso)performance requirements, $J_z(p_{iso}) = J_{z,req}$, are met one may consider competing cost objectives J_c (control effort, implementation cost, system mass, dissipated power, etc.) or risk objectives J_r (stability margins, sensitivity of performance to parametric uncertainty etc.). Which combination of J_c and J_r to use is application dependent.

In the NEXUS case a multivariable analysis was conducted for a subset of 10 out of the 25 design parameters from Table 1. The two performance objectives $J_{z,1}$ =RMMS WFE and $J_{z,2}$ =RSS LOS from above were used. The cost and risk objectives are defined as follows:

- $J_{c,1}$ = Build-to Cost, closeness of parameters to "mid-range", i.e. $(p_{UB} - p_{LB})/2$

- $J_{c,2}$ = FSM control gain, K_{fsm}

- $J_{r,1}$ = Percent performance uncertainty, $100 \cdot \Delta J_z / J_z$

Of these the first one is particularly interesting, since it can assist in finding a 'balanced' design. The assumption is that for all design parameters, p_j, there is a 'cheap' bound (easy to achieve with current state-of-the-art) and an 'expensive' bound (difficult to achieve with current state-of-the-art). For a given parameter p_j, either p_{LB} or p_{UB} will be the expensive bound. For the imbalances U_s, U_d it is clear that p_{LB} is more expensive (requires better balancing). If one can find a design that stays close to mid-range, i.e. i.e. $(p_{UB} - p_{LB})/2$, for parameters from different subsystems, then the burden for achieving the performance is shared and "fairly" distributed in the system. The three Pareto optimal solutions, which each individually optimize one of the above objectives, J_c, J_r, while meeting the isoperformance condition, are shown in the radar plot of Figure 9(a). Specifically, the isoperformance condition leads to the fact that all designs, p_A, p_B, p_C, asymptote to the same value in the cumulative RSS LOS plot in Figure 9(b).

The results for the NEXUS Pareto optimal designs are summarized in Table 3.

Table 3. NEXUS Pareto optimal designs

	$J_{z,1}$	$J_{z,2}$	$J_{c,1}$	$J_{c,2}$	$J_{r,1}$
A	20.0000	5.2013	**0.6324**	0.4668	± 14.3 %
B	20.0012	5.0253	0.8960	**0.0017**	± 8.8 %
C	20.0001	4.8559	1.5627	1.0000	± **5.3 %**
	[nm]	[μm]	[-]	[-]	[%]

Even though these designs A, B, C achieve the same WFE and LOS jitter performance, their dominant contributors in terms of disturbance sources are likely different. This leads naturally to the topic of error budgeting.
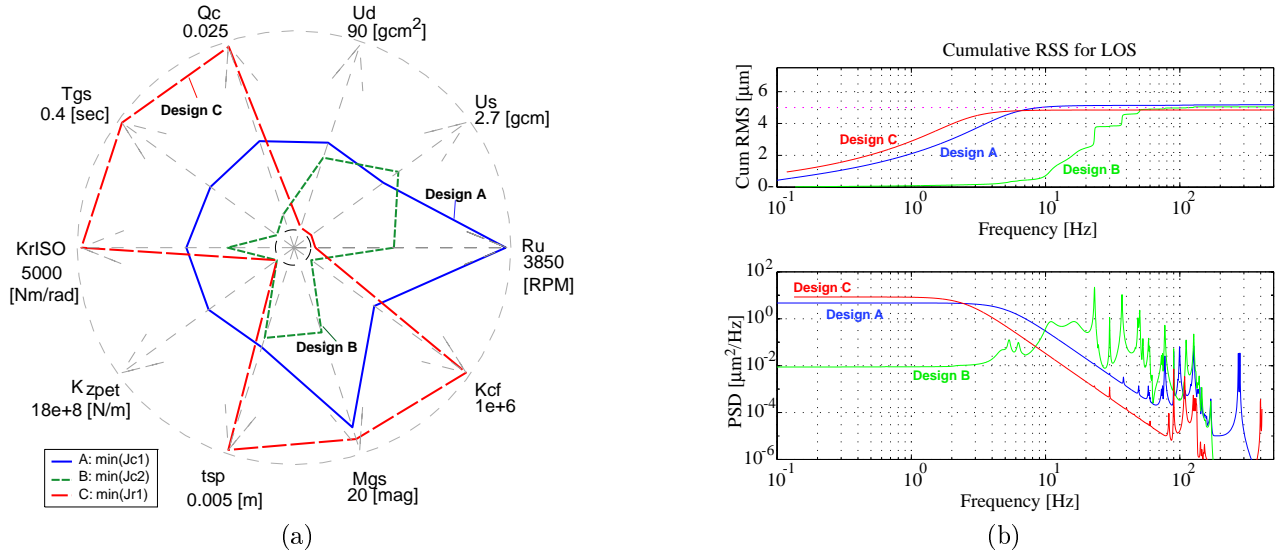
(a)

(b)

Figure 9. (a) NEXUS Multivariable Isoperformance. Radar plot of 3 Pareto optimal designs. $J_{c,1}$ is best mid-range design, $J_{c,2}$ is the design with smallest FSM gain, $J_{r,1}$ is the design with smallest performance uncertainty. (b) NEXUS Pareto Optimal Designs: RSS LOS power spectral densities (bottom) and cumulative RSS curves (top).

6. ERROR BUDGETING

Error budgeting finds the error contributions from all sources (e.g. RWA, sensor noises) and checks the feasibility of an apriori allocation ('error budget'). Figure 10(a) shows the apriori allocation (Budget), Ψ, and the actual disturbance contributions (Capability), Ψ^{**}, to the variance of RSS LOS for Design "A". This is the design that "balances" the burden between subsystems best. The error budget can be expressed in terms of the fractional contribution of the j-th disturbance source to the i-th performance as

$$\Psi_i = \sum_{j=1}^{n_d} \Psi_{i,j} = J_{z,req,i}^2 \tag{4}$$

The relative contributions to the performance can be shown by plotting the fractional contributions of the j-th error source on a hyper-sphere. This sphere is called the Error Sphere, see Figure 10(b), not showing ACS noise.
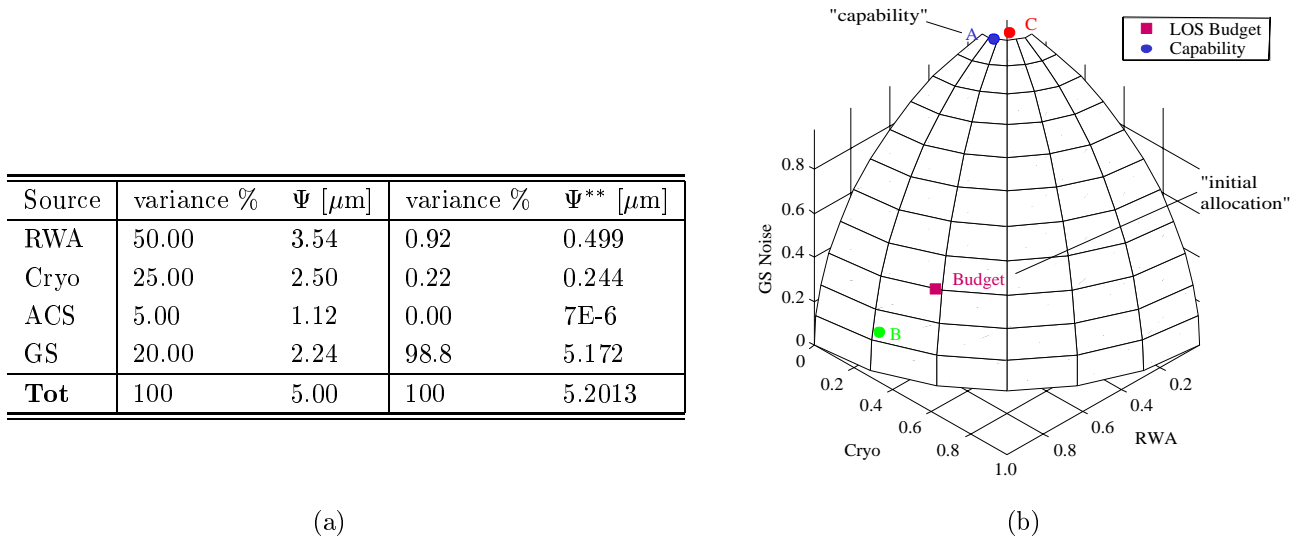
Source	variance %	Ψ [μm]	variance %	Ψ^{**} [μm]
RWA	50.00	3.54	0.92	0.499
Cryo	25.00	2.50	0.22	0.244
ACS	5.00	1.12	0.00	7E-6
GS	20.00	2.24	98.8	5.172
Tot	100	5.00	100	5.2013

(a)

(b)

Figure 10. (a) NEXUS error budget Ψ and actual capability Ψ^{**} for RSS LOS and design 'A', (b) NEXUS Error Sphere for RSS LOS. Note: ACS sensor noise contributions not shown.

We see that in the final design 'A' the jitter is dominated by guide star noise (limitation due to large guide star magnitude), whereas the initial design was dominated by reaction wheel noise. Error Budgeting is an obvious application of isoperformance, since an apriori error budget will always result in the desired performance level. The advantage of using isoperformance in this context is that a "capability" error budget, Ψ^{**}, can be found, which is theoretically achievable since it is based on the underlying integrated model.

7. SUMMARY

A comprehensive NEXUS Spacecraft analysis was conducted. It was demonstrated that the tight pointing and phasing requirements for the telescope can be achieved by a well "balanced" design that distributes the burden between the participating subsystems. NEXUS was chosen due to its interesting, flexible dynamics and the presence of important disturbance, plant, control and optics parameters. An disturbance and sensitivity analysis is conducted for an initial vector, p_o, of 25 design parameters. A bivariate isoperformance analysis traded dynamic wheel imbalance, U_d, versus isolator corner frequency, $K_r ISO$. A multivariable isoperformance analysis was conducted with 10 parameters. By applying cost and risk objectives, such as implementation cost (closeness to "mid-range"), smallest FSM control gain (K_{cf}) and smallest performance uncertainty, a set of three Pareto optimal designs was identified. The application of isoperformance to dynamics error budgeting is demonstrated by comparing an apriori allocation ("budget") with the error source contributions of a Pareto optimal design.

REFERENCES

1. D. W. Miller, O. L. de Weck, and G. E. Mosier, "Framework for multidisciplinary integrated modeling and analysis of space telescopes," in *First International Workshop on Integrated Modeling of Telescopes SPIE/ESO*, (Lund, Sweden), 5-7 February 2002.

2. O. de Weck, *Multivariable Isoperformance Methodology for Precision Opto-Mechanical Systems*. PhD thesis, Massachusetts Institute of Technology, 77 Mass Ave, Cambridge, MA 01760, June 2001.

3. Jet Propulsion Laboratory, *Integrated Modeling of Optical Systems User's Manual*, January 1998. JPL D-13040.

4. D. C. Redding and W. G. Breckenridge, "Optical modeling for dynamics and control analysis," *Journal of Guidance, Control, and Dynamics* **14**, pp. 1021–1032, Sept.-Oct. 1991.

5. F. Liu, "NEXUS Optical Sensitivities," Tech. Rep. NEXUS:99-007, Swales Aerospace & Associates Inc., 5050 Powder Mill Road, Beltsville, MD 20705, December 1999.

6. R. A. Masterson, D. W. Miller, and R. L. Grogan, "Development and validation of reaction wheel disturbance models: Empirical model," *Journal of Sound and Vibration* **249**, pp. 575–598, March 2002.

7. B. Bialke, "A compilation of reaction wheel induced spacecraft disturbances," in *Proceedings of the 20th Annual AAS Guidance and Control Conference*, (Breckenridge, CO), February 5–9, 1997. AAS Paper No. 97-038.

8. H. L. Gutierrez, *Performance Assessment and Enhancement of Precision Controlled Structures During Conceptual Design*. PhD thesis, Massachusetts Institute of Technology, Department of Aeronautics and Astronautics, 1999.

9. J. Spanos, Z. Rahman, and G. Blackwood, "A soft 6-axis active vibration isolator," in *Proceedings of the American Control Conference*, (Seattle, WA), June 1995.

10. O. de Weck, *Multivariable Isoperformance Methodology for Precision Opto-Mechanical Systems*. PhD thesis, M.I.T., August 2001.

11. O. L. de Weck, S. Uebelhart, H. Gutierrez, and D. Miller, "Performance and sensitivity analysis for large order linear time-invariant systems," in *9th AIAA/ISSMO Symposium on Multidisciplinary Analysis & Optimization*, (Atlanta, Georgia), 4-6 Sept 2002. Paper AIAA-2002-5437.